Journal of Immunological Methods 468 (2019) 61–66

Contents lists available at ScienceDirect

Journal of Immunological Methods

journal homepage: www.elsevier.com/locate/jim

Technical Note

A standardised protocol for the evaluation of small extracellular vesicles in plasma by imaging flow cytometry

Armitage J.D.[a,b,*], Tan D.B.A.[a,b], Cha L.[b], Clark M.[a,c], Gray E.S.[c], Fuller K.A.[a,d], Moodley Y.P.[a,b,e]

[a] School of Biomedical Sciences, University of Western Australia, Perth, WA, Australia
[b] Stem Cell Unit, Institute for Respiratory Health, Perth, WA, Australia
[c] School of Medical and Health Sciences, Edith Cowan University, Perth, WA, Australia
[d] PathWest Laboratory Medicine, WA, Australia
[e] Department of Respiratory Medicine, Fiona Stanley Hospital, Murdoch, WA, Australia

ARTICLE INFO

Keywords:
Extracellular vesicles
Imaging flow cytometry
Extracellular vesicles
Immunophenotyping
Swarm detection

ABSTRACT

Flow cytometry provides robust, multi-parametric and quantitative information on single cells which also exhibits enormous potential as a tool for small particle characterisation. Small extracellular vesicle (sEV) detection by flow cytometry remains compromised due to the high prevalence of swarm detection, which is defined by the simultaneous illumination of more than one sEV, recorded as a single event. Detection of sEVs by imaging flow cytometry presents a major advantage by having the ability to resolve single particles from swarm detection based on the image features recorded for each event. In this study, we provide a simplified protocol that facilitates the removal of both swarm events and aggregated particles to improve the accuracy of sEV analysis. Our results indicate that imaging flow cytometry should be at the forefront as a robust and sensitive technique for sEV characterisation.

1. Introduction

Small extracellular vesicles (sEVs) vary from 30 to 200 nm in size, and are enriched in a variety of bioactive molecules and surface markers including CD9, CD63, CD81 and tumour suppressor gene (TSG)-101 (Raposo and Stoorvogel, 2013). SEVs arise from several sources during health and disease and may serve as biomarkers of pathological processes as well as providing options for delivery of therapeutic cargoes to sites of injury (Inamdar et al., 2017). However, despite significant research there are major challenges in standardising methods to quantify and characterise sEVs.

Single sEV flow cytometry has the potential to provide rapid quantitative data on sEVs based on their surface expression, however there are still unresolved limitations surrounding the sensitivity of the technique due to the low refractive index of sEVs (Gardiner et al., 2014). Furthermore, the accuracy of flow-based characterisation becomes compromised due to the prevalence of coincident sEV ("swarm") detection, which describes the phenomenon where more than one particle is detected at the same time, processing it as a single event (Van Der Pol et al., 2012).

The Amnis ImageStream®[X] Mark II imaging flow cytometer (ISXmkII) combines the use of conventional flow cytometry with fluorescent microscopy. The ISXmkII possesses a host of components which improves small particle detection, including stronger excitation lasers (100–200 mW) charged couple device detectors, time delay integration, and ultra-precise fluidics. For these reasons, the use of the ISXmkII has become a well described method for flow-based sEV quantification (Erdbrügger et al., 2014; Headland et al., 2014; Lannigan and Erdbruegger, 2017; Mastoridis et al., 2018). Despite the advances of sEV flow cytometry, challenges still remain. At present, gating strategies cannot discriminate single particles versus. Multiple particles based on conventional fluorescent or scatter parameters. The most unique feature of the ISXmkII, is its ability to capture high resolution images of every recorded event which provides positional information of the fluorescence within the image. Such images possess the potential to discriminate swarm from single particles (i.e. multiple fluorescent positions versus. a single fluorescent position within the image). The use of this advantage remains underutilised for EV work.

One of the biggest limitations surrounding the use of flow cytometry for EV analysis is a lack of standardised protocols that can be easily replicated. This study provides a simplified protocol that can be utilised to rapidly quantitate single sEV particles from either clarified (filtered,

* Corresponding author at: School of Biomedical Sciences, University of Western Australia, Rear 50 Murray Street, Level 2 Medical Research Foundation, Royal Perth Hospital, Perth, WA 6000, Australia.
E-mail address: jesse.armitage@research.uwa.edu.au (J.D. Armitage).

https://doi.org/10.1016/j.jim.2019.03.006
Received 31 August 2018; Received in revised form 5 February 2019; Accepted 14 March 2019
Available online 16 March 2019
0022-1759/

platelet-poor) plasma or sEVs isolated and enriched by size-exclusion chromatography while accurately quantifying EVS through the exclusion of swarm detection. This would be an important methodological advancement in understanding sEV physiology and pathology.

2. Materials and methods

2.1. Isolation of plasma-derived sEVs

Lithium heparin plasma was first clarified by serial low speed centrifugation (2000 xg; 10 mins and 10,000 xg; 30 mins) followed by 0.22 μm centrifugal filtration (14,000 xg; 2 mins) at room temperature (RT). Clarified plasma (500 μL) was carefully applied to a qEV column (Izon Sciences, Christchurch, NZ) which is a size-exclusion chromatography column. Elution buffer (sterile, 0.22 μm-filtered phosphate-buffered saline; PBS; Sigma-Aldrich, Castle Hill, NSW, Australia) is sequentially added until 3 mL of total volume has passed through the column (fractions 1–6 at 500 μL per fraction). Fractions 7–9 (1.5 mL) were then collected for sEV enrichment by concentrating the sEV fraction using a 100 kDa molecular weight cutoff filter device (Merck Millipore, Burlington, MA, USA) to achieve a final volume of 50 μL.

2.2. Visualisation of sEVs by transmission electron microscopy (TEM)

SEVs resuspended in PBS were transferred onto 200 mesh Formvar®-carbon coated copper grids (ProSciTech, Kirwan, QLD) and adsorbed for 15 mins at room temperature. Excess suspension was blotted off using Whatman® no. 1 filter paper following incubation. After blotting off excess suspension, grids were fixed with 1% glutaraldehyde in PBS for 5 min, washed a further 8 times and contrasted using 0.5% uranyl acetate/H_2O for 2 min. Excess stain was blotted off thoroughly and grids were dried for at least 2 days. Grids were visualised on the JEOL JEM-2100 electron microscope (JEOL, Tokyo, Japan) at an operating voltage of 80 kV. Images were captured using an 11 M pixel Gatan Orius digital camera.

2.3. Visualisation and analysis of sEVs by Nanoparticle Tracking Analysis (NTA)

The concentration and size distribution of particles in collected fractions was measured with NTA coupled with the NanoSight syringe pump (NS300; Nanosight, Amesbury, UK), equipped with a sCMOS camera and a 405 nm diode laser. Pooled and concentrated qEV fractions (7–9), were pre-diluted 1:20 in PBS prior to acquisition, before being loaded into a 1 mL syringe. Measurement was performed during a syringe pump speed of 200 μL/min, where 3 videos, each of 60-s duration were captured with the slider shutter set at 1200 and the camera gain set at 370. Analysis was performed by the instrument software (NTA 3.3.104).

2.4. Western blotting of sEV samples

SEVs (in PBS) were added 1:1 to radioimmunoprecipitation (RIPA) assay buffer containing a complete protease inhibitor tablet (Roche, Basel, Switzerland) and incubated for 30 mins on ice. Samples were then diluted 1:4 in Lamelli Buffer (Bio-Rad, Hercules, CA, USA). Proteins were separated on a mini TGX 5–15% stain free gel (Bio-Rad). Proteins were then transferred onto a nitrocellulose blotting membrane using the trans-blot® Turbo™ transfer system (Bio-Rad). The membrane was probed using the iBind Flex western device (SLF2000; Thermofisher, Wilmington, DE). The membrane was blocked for 20 min in iBind Flex solution (SLF2020; Thermofisher) followed by incubations with either 4 μg/mL negative marker calnexin (Novus Biologicals, Littleton CO, USA), 0.2 μg/mL CD81 or 0.8 μg/mL CD9 (Thermofisher). Membranes were then incubated with sheep anti-mouse IgG conjugated to horse radish peroxidase (HRP, 1:2000; GE Healthcare, UK). Signals were developed using clarity ECL blotting substrates (Bio-Rad) and were subsequently imaged using the ChemiDoc Touch Imaging System (Bio-Rad). Images were processed using Image Lab (Bio-Rad).

2.5. Flow cytometer setup and fluorescent labelling

Imaging flow cytometry was performed using the ISXmkII with INSPIRE v4.1 acquisition software (AMNIS Millipore Sigma, Seattle, USA). Three excitation lasers were utilised for fluorescence detection: 120 mW 405 nm (violet), a 200 mW 488 nm (blue) and 150 mW 642 nm (red) solid state lasers. A 70 mW 785 nm laser was used to provide side-scatter (SSC) signal and detect SpeedBeads™ for internal calibration. All images were captured using a 60 × objective brightfield camera with extended depth of field enabled. All sEV acquisitions used the lowest flow rate setting to provide maximum sensitivity.

The following antibody staining protocol was adapted from Headland et al. (Headland et al., 2014). Briefly, 20 μL of purified sEVs or clarified plasma were initially blocked with 2.5 μg of FcR blocking reagent (BD Biosciences, San Jose, USA) for 10 min at room temperature. A CD9-PE and CD81-APC (BD Biosciences) cocktail was initially prepared by 0.22 μm centrifugal filtration (14,000 xg; 30 s) to remove antibody aggregates. Cocktail was then added to the sEV sample to achieve a final concentration of 1.25 μg/mL for both CD9-PE and CD81-APC, and incubated for 30 min at room temperature. Equivalent concentrations of the respective isotype controls were added to determine the degree of non-specific binding. Labelled samples were then assayed immediately by the ISXmkII cytometer. Validation of vesicle detection was determined by a post-labelling treatment by 5% triton X-100 (5 μL), followed by a 30 min incubation prior to imaging.

All sEV data analysis was performed using IDEAS v6.0 imaging software. Using the IDEAS software, an image mask was generated to combine the image features in the CD9-PE and CD81-APC channels to perform an additional calculation: spot count (SC), which is an enumeration of discrete fluorescent regions within the images field of view (Jenner et al., 2016) which was employed to enumerate the number of EV particles detectable within the image. A schematic of the workflow and the setup steps on the IDEAS software is shown in Fig. 1. In summary this workflow creates an image mask that merges information from Ch03 and Ch11. Performing a spot count on this image mask can then enumerate the discrete fluorescent regions within both Ch03 and Ch11.

3. Results

3.1. SEV validation and characterisation by imaging flow cytometry

Plasma-derived sEVs were purified by qEV and quantitated by NTA (modal particle diameter of ~80 nm). A representative image displays the visualisation of particles during sample acquisition (Fig. 2a). Visual confirmation was perform by TEM showing the presence of nanoparticles around 100 nm in qEV preparations (Fig. 2b). Western blots also confirm the presence of a $CD9^+CD81^+$Calnexin- sEV fraction (Fig. 2c). To remove Speedbeads from the analysis, which are used to calibrate the instrument, sEV events were first gated on a low side-scatter (SSC) of $< 10^3$ (Fig. 2d). A spot count feature was then applied to all low SSC events to quantitate single particles (Fig. 2e). Representative images from each gate show the presence of swarm events with a spot count > 1 (Fig. 2f). A series of tests were individually performed to validate the detection of EV particles following qEV isolation (Fig. 2g, left to right): (1) Double staining of CD9-PE and CD81, (2) Double staining using respective isotype controls to determine degree of non-specific binding, (3) a CD9-PE and CD81-APC single stain control to assist in gate placement, and (4) a lysis control to confirm the membranous nature of detectable particles. Antibodies diluted in PBS in the absence of EVs were also acquired to determine the absence of free antibody detection (Fig. 2h). Representative images of each EV

A

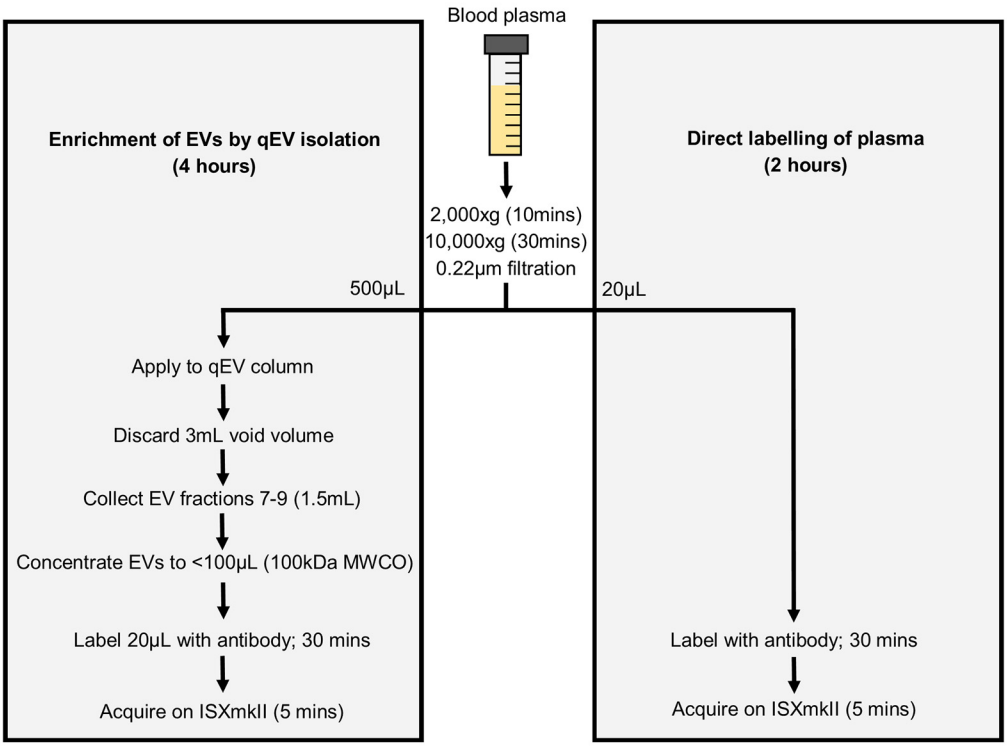

B

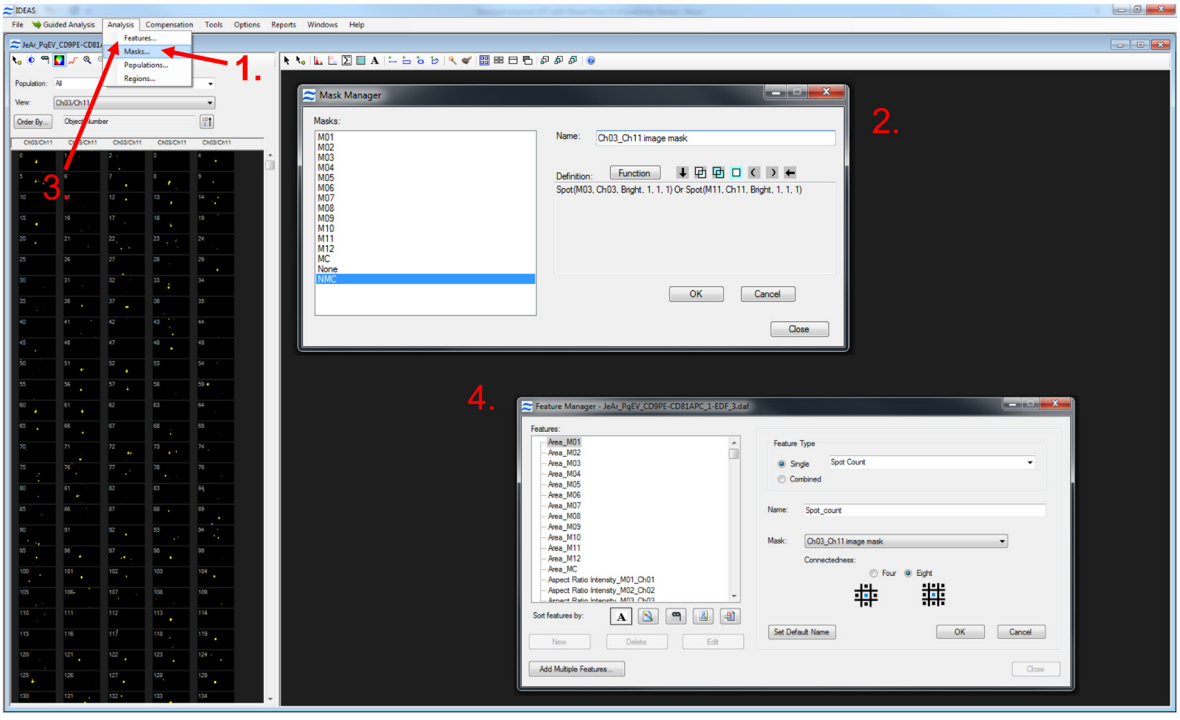

Fig. 1. Sample preparation and setup of analysis using the IDEAS software. A schematic showing the processing steps when characterising EVs either after qEV enrichment or directly from plasma (A). Setup of IDEAS software for the analysis of single EVs in samples recorded by the ISXmkII (B): 1-Select "Masks" under the Analysis tab to open the image masks window. 2-Create a new image mask that merges ("or" function) both Ch03 (CD9-PE) and Ch11 (CD81-APC) together. 3-Open "Features" under the analysis table 4-Create a new feature by using the dropdown menu to select "Spot Count". Select the merged image mask to create a new image feature quantitating spot count using the merged image mask.

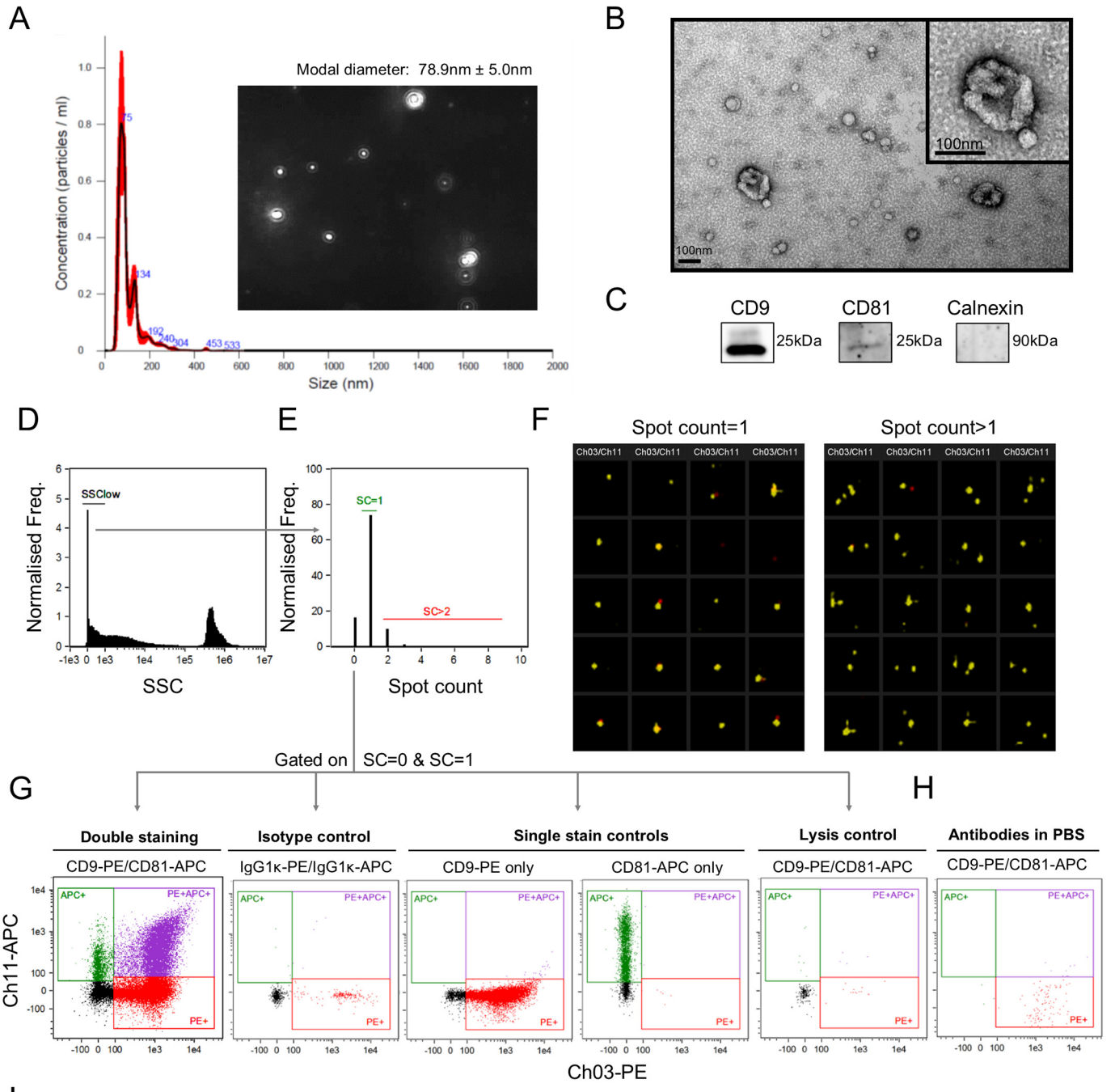

(caption on next page)

Fig. 2. Validation of EVs by conventional methods and imaging flow cytometry. Triplicate EV measurements made on the nanosight (including a representative image of 1 of the 3 video captures) show a modal particle diameter of ~80 nm (A) Representative TEM images show the presence of EV-like structures with the characteristic size and morphology (B), while western blotting shows expression of tetraspanins CD9 and CD81 with an absence of negative marker Calnexin (C). SEVs were first gated for low SSC (D), followed by a spot count of < 1 (E). Representative images verify the presence of swam detection with a spot count > 1 (F). Various controls were employed to validate the detection and staining of EV-like particles with positivity for CD9 and/or CD81 including isotype, single stain and lysis controls (G). Free antibody detection (antibodies without EVs) was also measured (H). Representative images of events captured for each EV population are shown (I).

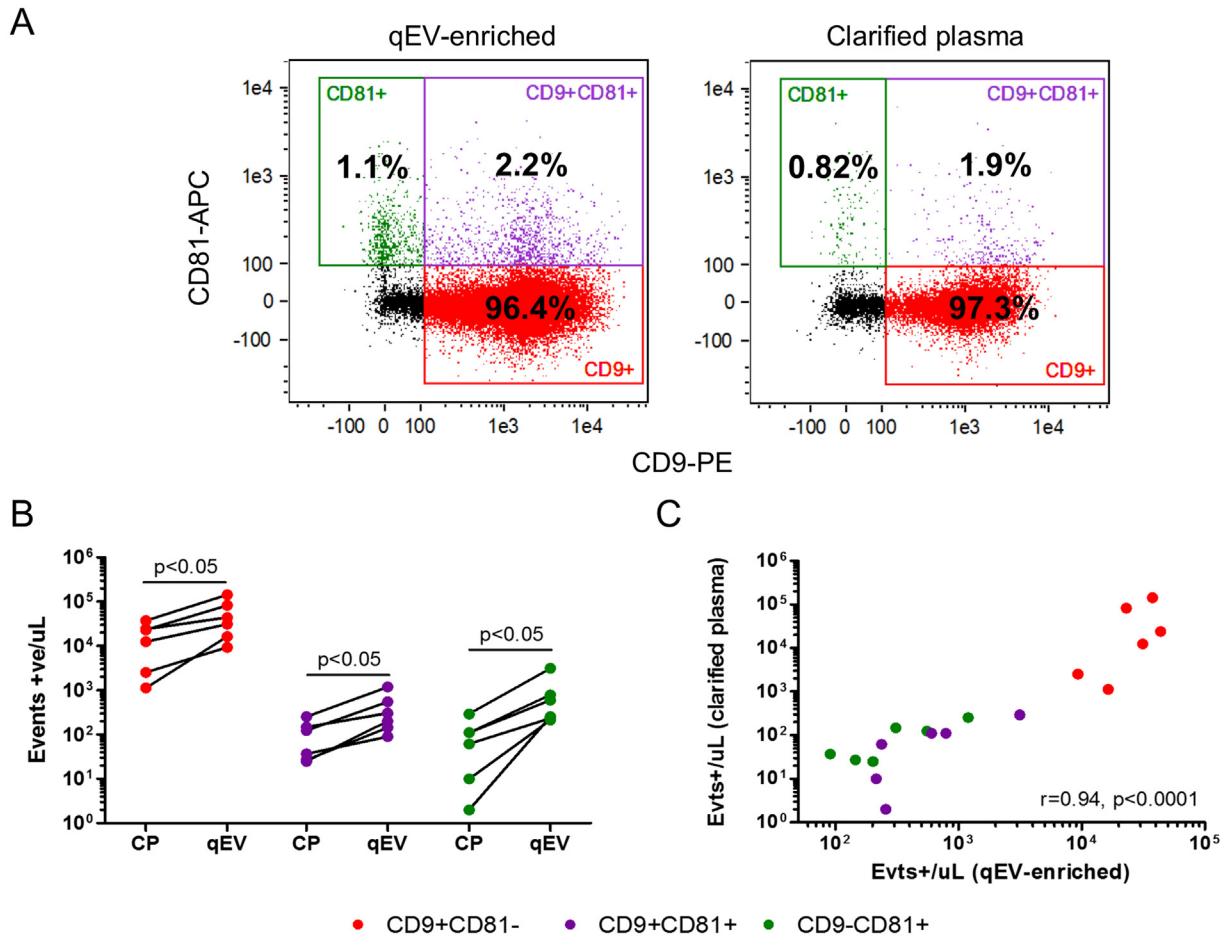

Fig. 3. Comparison of EV quantification before and after qEV enrichment. $CD9^+CD81^-$, $CD9^-CD81^+$, $CD9^+CD81^+$ EV subsets directly quantitated from plasma or after qEV enrichment showed similar proportions by ISXmkII (A). Enrichment of plasma sEVs by qEV significantly improved the detectability of EV subsets (B), while concentrations of EV subsets in plasma strongly correlated with concentrations measured after qEV enrichment (C).

populations of $CD9^+CD81^-$ $CD9^-CD81^+$ and $CD9^+CD81^+$ are also shown as confirmation.

3.2. EVs can be quantitated directly from plasma or following EV enrichment

EVs were quantitated from six healthy controls either directly from plasma, (20 µL) or following enrichment of EVs using qEV columns (500 µL starting plasma). Representative plots from 1 individual show the similarity in distribution of EV subsets with various staining for CD9-PE and CD81-APC (Fig. 3a). Comparatively, qEV enrichment significantly improved the detection of these EV phenotypes (Fig. 3b). These levels also strongly correlated with each other (Fig. 3c; $p < 0.0001$; $r = 0.94$).

4. Discussion

The ISXmkII has been proposed as the preferred platform for performing sensitive measurements by flow cytometry due to its specialised features. Thus, it has been implicated as a useful diagnostic and prognostic tool, particularly in a cancer context (Doan et al., 2018). The ISXmkII has been used in a number of applications related to EVs, which includes the study of interactions between EVs and target cells (Ofir-Birin et al., 2018; Ohno et al., 2013), the subsetting of EVs in plasma based on their surface expression (Headland et al., 2014).

Mastoridis et al. has demonstrated that events detectable by the ISXmkII are indeed sEVs using the appropriate controls, particularly a lysis control which confirms the membranous nature of detectable events (Mastoridis et al., 2018). While methods are established to validate the presence of sEVs by the ISXmkII, swarm detection and misinterpretation of aggregated sEVs are a major source of erroneous analysis in sEV characterisation, leading to the under-estimation of sEV concentrations and generation of false positives (Van Der Pol et al., 2012). It appears that erroneous detection is inevitable when assaying samples with a high EV concentration (such as plasma). We demonstrate that with the use of spot counting to filter out swarm detection, samples can still be acquired at a reasonable rate without the need of excessive dilution. Indeed, the use of imaging features to exclude

coincident detection has been previously described using the “delta centroid” parameter (defined as the distance between the centroid feature measured in 2 channels), where swarm events were identified as having a high delta centroid. In some circumstances, this feature is not suitable for EV analysis as it cannot identify swarm events that only contain positivity for a single marker as it relies on the centroid measurement in 2 channels. Secondly, the study also requires manual selection of true/false positives populations, which potentially introduces user bias and more hands-on time (Lannigan and Erdbruegger, 2017). We propose that a novel gating using the spot count image feature is a more robust and simplified methodology for the removal of swarm events from imaging flow analysis.

One of the key advantages of this methodology is the rapid staining and quantification of EVs without the need to wash off free antibody that is not EV-bound. This enables the quantification of EVs directly from plasma (despite the presence of protein contaminants) within 2 h. Moreover, we show that this protocol is also compatible with EV enrichment techniques which may improve the detectability of less abundant EV phenotypes. In this study, we utilised 2 common EV markers belonging to the tetraspanin family (CD9 and CD81). Although these are known to be highly enriched in EV preparations, these was a major discrepancy in the levels of $CD9^+$ and $CD81^+$ EV particles in plasma. Therefore, detectability of $CD81^+$ EVs (and more so $CD9^+CD81^+$ EVs which were even less abundant) demonstrates the compatibility of this protocol with the detection of EV related antigens that may be less abundant.

For this study we chose to use qEV isolation, a commercially available isolation kit that employs size exclusion chromatography to purify sEVs around within the accepted size range 30-200 nm. It has been demonstrated that the purity of plasma-derived EVs after qEV enrichment is superior compared to alternative isolation methods. Moreover, this isolation method does not involve pelleting or high speed aggregation which may induce aggregation of EVs, and other contaminants (Lobb et al., 2015). To our knowledge, no imaging flow cytometry based protocol utilises qEV-isolated EVs, however we demonstrate that qEV enrichment can not only improve the detection of low abundance EVs, but also preserves the relative proportions of EV subsets measured directly from plasma.

In conclusion, we have outlined a flow-based protocol that incorporates a novel gating strategy using the spot count feature, and a rapid staining protocol can provide robust quantification of EVs following qEV isolation and also directly in plasma. The ISXmkII possesses enormous potential and should be at the forefront of techniques employed to characterise sEVs due to their unique advantages in sensitivity and accuracy.

Funding

This research did not receive any specific grant from funding agencies in the public, commercial, or not-for-profit sectors.

Conflict of interest

All authors have no conflict of interest to declare.

Acknowledgements

The authors thank all healthy donors used in this study. The authors also acknowledge the facilities, and the scientific and technical assistance of the Australian Microscopy & Microanalysis Research Facility at the Centre for Microscopy, Characterisation & Analysis, University of Western Australia, a facility funded by the University, State and Commonwealth Governments. This study was supported by funding a National Health and Medical Research Council grant. The authors also thank Dr. Katie Meehan at the Translation Cancer Pathology Laboratory, University of Western Australia for technical assistance with the Nanosight instrument.

References

Doan, M., Vorobjev, I., Rees, P., Filby, A., Wolkenhauer, O., Goldfeld, A.E., Lieberman, J., Barteneva, N., Carpenter, A.E., Hennig, H., 2018. Diagnostic potential of imaging flow Cytometry. Trends Biotechnol. 36, 649–652.

Erdbrügger, U., Rudy, C.K., Etter, E., Dryden, M., Yeager, K.A., Klibanov, M., Lannigan, A.L.J., 2014. Imaging flow cytometry elucidates limitations of microparticle analysis by conventional flow cytometry. Cytometry Part A 85, 756–770.

Gardiner, C., Shaw, M., Hole, P., Smith, J., Tannetta, D., Redman, C.W., Sargent, I.L., 2014. Measurement of refractive index by nanoparticle tracking analysis reveals heterogeneity in extracellular vesicles. J. Extracell. Vesicles 3, 25361.

Headland, S.E., Jones, H.R., D'sa, A.S.V., Perretti, M., Norling, L.V., 2014. Cutting-edge analysis of extracellular microparticles using ImageStreamX imaging flow Cytometry. Sci. Rep. 4, 5237.

Inamdar, S., Nitiyanandan, R., Rege, K., 2017. Emerging applications of exosomes in cancer therapeutics and diagnostics. Bioeng. Transl. Med. 2, 70–80.

Jenner, D., Ducker, C., Clark, G., Prior, J., Rowland, C.A., 2016. Using multispectral imaging flow cytometry to assess an in vitro intracellular Burkholderia thailandensis infection model. Cytometry Part A 89, 328–337.

Lannigan, J., Erdbruegger, U., 2017. Imaging flow cytometry for the characterization of extracellular vesicles. Methods 112, 55–67.

Lobb, R.J., Becker, M., Wen, S.W., Wong, C.S.F., Wiegmans, A.P., Leimgruber, A., MÖller, A., 2015. Optimized exosome isolation protocol for cell culture supernatant and human plasma. J. Extracell. Vesicles 4 (27031–27031).

Mastoridis, S., Bertolino, G.M., Whitehouse, G., Dazzi, F., Sanchez-Fueyo, A., Martinez-Llordella, M., 2018. Multiparametric analysis of circulating Exosomes and other small extracellular vesicles by advanced imaging flow Cytometry. Front. Immunol. 9.

Ofir-Birin, Y., Abou Karam, P., Rudik, A., Giladi, T., Porat, Z., Regev-Rudzki, N., 2018. Monitoring extracellular vesicle cargo active uptake by imaging flow Cytometry. Front. Immunol. 9, 1011.

Ohno, S.-I., Takanashi, M., Sudo, K., Ueda, S., Ishikawa, A., Matsuyama, N., Fujita, K., Mizutani, T., Ohgi, T., Ochiya, T., Gotoh, N., Kuroda, M., 2013. Systemically injected Exosomes targeted to EGFR deliver antitumor MicroRNA to breast Cancer cells. Mol. Ther. 21, 185–191.

Raposo, G., Stoorvogel, W., 2013. Extracellular vesicles: exosomes, microvesicles, and friends. J. Cell Biol. 200, 373.

Van Der Pol, E., Van Gemert, M.J., Sturk, A., Nieuwland, R., Van Leeuwen, T.G., 2012. Single vs. swarm detection of microparticles and exosomes by flow cytometry. J. Thromb. Haemost. 10, 919–930.